

# In vivo kinetic approach reveals slow SOD1 turnover in the CNS

Matthew J. Crisp, Kwasi G. Mawuenyega, Bruce W. Patterson, Naveen C. Reddy, Robert Chott, Wade K. Self, Conrad C. Weihl, Jennifer Jockel-Balsarotti, Arun S. Varadhachary, Robert C. Bucelli, Kevin E. Yarasheski, Randall J. Bateman, and Timothy M. Miller

Washington University School of Medicine, St. Louis, Missouri, USA.

Therapeutic strategies that target disease-associated transcripts are being developed for a variety of neurodegenerative syndromes. Protein levels change as a function of their half-life, a property that critically influences the timing and application of therapeutics. In addition, both protein kinetics and concentration may play important roles in neurodegeneration; therefore, it is essential to understand in vivo protein kinetics, including half-life. Here, we applied a stable isotope-labeling technique in combination with mass spectrometric detection and determined the in vivo kinetics of superoxide dismutase 1 (SOD1), mutation of which causes amyotrophic lateral sclerosis. Application of this method to human SOD1-expressing rats demonstrated that SOD1 is a long-lived protein, with a similar half-life in both the cerebral spinal fluid (CSF) and the CNS. Additionally, in these animals, the half-life of SOD1 was longest in the CNS when compared with other tissues. Evaluation of this method in human subjects demonstrated successful incorporation of the isotope label in the CSF and confirmed that SOD1 is a long-lived protein in the CSF of healthy individuals. Together, the results of this study provide important insight into SOD1 kinetics and support application of this technique to the design and implementation of clinical trials that target long-lived CNS proteins.

## Introduction

Amyotrophic lateral sclerosis (ALS) is an adult-onset neurodegenerative disorder characterized by the loss of motor neurons in the spinal cord and cortex, resulting in progressive paralysis and death on average 2–3 years after symptom onset (1). With an incidence of 1.5 to 2.7 cases per 100,000 in North America and Western Europe, ALS is the third most common neurodegenerative disorder after Alzheimer's and Parkinson's diseases and the most common motor neuron disease (2). Almost universally fatal, the only FDA-approved drug for ALS is riluzole, a nonspecific NMDA receptor antagonist that prolongs survival by 2 to 4 months (3). Moving forward, therapies that specifically target the proteins responsible for familial forms of ALS are being developed. For these and other targeted therapies in neurodegenerative disease, quantification of protein kinetics (half-life, production, and clearance) is a key factor in optimizing the fre-

quency of delivery and determining the optimal time to assess for a biological response.

Measurement of protein turnover has been routinely conducted in cell culture with radioisotopes that have provided important information regarding how protein characteristics (mutations, conformations, and posttranslational modifications among others) affect protein turnover. However, measuring turnover rates of proteins in an immortalized, rapidly dividing cell culture model has limitations and shows discrepancies when turnover rates of identical proteins are compared between tissues and cell culture models (4). The development of stable isotope-labeling kinetics (SILK) has enabled the study of protein turnover rates in vivo using a safe, stable isotope amino acid tracer that is incorporated into newly synthesized proteins and can be quantitatively measured by mass spectrometry — a technique that has been highly successful in studies of amyloid- $\beta$  in human cerebral spinal fluid (CSF) and in brains from animal models (5–12). In these studies, a relatively short (9-hour) intravenous infusion of the stable isotope  $^{13}\text{C}_6$ -leucine resulted in adequate labeling of the rapidly turned over amyloid- $\beta$  (half-life of 8 hours). However, the measurement of the turnover of long-lived proteins is challenging, especially in humans. The labeling time needed becomes too long for an intravenous approach, and sample collection must be carried out over many days instead of hours. Indeed,  $\text{D}_2\text{O}$ -labeling studies in both animal models and human subjects have demonstrated that long-term labeling is necessary to measure proteins with a half-life on the order of days (13, 14). Here, we report the development of a SILK method using a stable isotope-labeled amino acid to measure the turnover of a long-lived protein in rodents and in human CSF.

We applied our SILK method first to superoxide dismutase 1 (SOD1), a homodimeric metalloenzyme that catalyzes the conver-

**Conflict of interest:** Timothy M. Miller receives research support from Biogen and Isis Pharmaceuticals Inc. and research reagents from Regulus Therapeutics. Timothy M. Miller served on a medical advisory board for Biogen and for Isis Pharmaceuticals Inc. Washington University, with Randall J. Bateman and Timothy M. Miller as coinventors, has submitted the US nonprovisional patent application "Metabolism of SOD1 in CSF" (docket 011873-PCT1/1). C2N Diagnostics has licensed intellectual property associated with this patent. Washington University and Randall J. Bateman have a financial interest in C2N Diagnostics, which uses the SILK methodology in human studies. C2N Diagnostics did not support this work. Randall J. Bateman is coinventor on US patent 7,892,845 "Methods for measuring the metabolism of neurally derived biomolecules in vivo" assigned to Washington University. Randall J. Bateman has consulted for Roche, Lilly, Boehringer Ingelheim, and FORUM Pharmaceuticals and has received research grants from Lilly and Roche in the past year. Conrad C. Weihl received research funds from Ultragenyx Pharmaceuticals Inc. **Submitted:** January 2, 2015; **Accepted:** May 7, 2015.

**Reference information:** *J Clin Invest.* 2015;125(7):2772–2780. doi:10.1172/JCI80705.

sion of superoxide anion to hydrogen peroxide and molecular oxygen (15, 16). Mutations in SOD1 cause dominantly inherited ALS via a toxic gain of function. Recent work by our group using antisense oligonucleotides (ASOs) against *SOD1*, a gene responsible for 20% of familial ALS cases, has shown great promise in animal models and has recently completed a phase I clinical trial (17). Our work and that with other targeted therapies highlight the need to understand SOD1 kinetics in order to effectively design clinical trials (17–21). Specifically, half-life determines the predicted nadir for SOD1 levels in the CSF of patients treated with protein production inhibitors. Since SOD1 CSF levels correlate with SOD1 levels in the CNS, measurement of SOD1 CSF protein in humans offers the ability to determine pharmacodynamics for future clinical trial design (22). We first developed our SILK method in rats expressing human SOD1 protein, in which we successfully measured the half-life of SOD1 in tissues and in the CSF. Translating our findings in rats to human CSF demonstrated excellent labeling of SOD1, defined the half-life of SOD1 in humans, and further validated this method for using stable isotopes to measure turnover of long-lived proteins.

## Results

*Development of  $^{13}\text{C}_6$ -leucine-labeling approach and mass spectrometry-based method for quantifying labeled SOD1 in cell culture.* The calculation of protein turnover by administering stable isotope-labeled amino acids or  $\text{D}_2\text{O}$  over time has been demonstrated in numerous cell culture models and in human CSF and plasma proteins (5–14, 23). Stable isotope-labeled amino acids are biologically identical to their naturally occurring counterparts and, unlike radiolabeled amino acids, are innocuous to both the system being studied and the experimental environment. SILK uses the administration of a stable isotope-labeled amino acid that is incorporated during protein translation. The labeled and unlabeled proteins are immunoprecipitated, digested into peptides, and analyzed using liquid chromatography and tandem mass spectrometry (LC/tandem MS) to quantify incorporation of the tracer into specific peptides (Figure 1, A and B). Using  $^{13}\text{C}_6$ -leucine-labeled HEK293T cells, we identified 3 leucine-containing peptides that reliably and accurately determined incorporation of label (Figure 1, C–E, and Supplemental Figure 1; supplemental material available online with this article; doi:10.1172/JCI80705DS1). These data confirmed our ability to label, isolate, and measure tracer-incorporated SOD1 using LC/tandem MS.

*Development of a SILK method to measure SOD1 turnover in vivo.* Preliminary experiments revealed insufficient labeling in human CSF SOD1 during a 9-hour intravenous infusion of  $^{13}\text{C}_6$ -leucine (data not shown). Based on this observation, we concluded that CSF SOD1 half-life in vivo was likely on the order of days to weeks rather than hours. To develop the method, we labeled human SOD1-expressing rats by oral administration of  $^{13}\text{C}_6$ -leucine. We used rats expressing either WT human SOD1 or mutant human SOD1 G93A protein, a well-studied mutation that is known to cause ALS in humans and is characterized by a predictable disease onset in animal models (24, 25). Approximately 100-day-old transgenic rats overexpressing human SOD1 WT or G93A were orally administered  $^{13}\text{C}_6$ -leucine for 7 days, followed by unlabeled leucine for an additional 56 days. Plasma, spinal cords, cortices, CSF, livers, and kidneys were collected at indicated time points (Figure 2A) in order to model plasma-free  $^{13}\text{C}_6$ -leucine and SOD1 kinetics

in vivo. Following detergent fractionation to immunoprecipitate soluble SOD1 from tissues, we used our LC/tandem MS method to detect and analyze leucine-containing SOD1 peptides and quantify SOD1 fractional turnover rates (FTRs) and half-life in each tissue.

The shape of the plasma-free  $^{13}\text{C}_6$ -leucine curve followed a pseudo linear increase during the oral  $^{13}\text{C}_6$ -leucine pulse and first-order kinetic decay during the chase with unlabeled leucine (Figure 2B). This confirmed that our oral labeling approach achieved sufficient  $^{13}\text{C}_6$ -leucine incorporation into soluble SOD1 peptides, with minimal variance among animals. The SOD1-labeling curves reflect tracer derivation from a direct precursor/product relationship between plasma leucine and each protein, as the SOD1-labeling curves intersect the plasma leucine enrichment at their peak enrichments (Figure 2B). These measurements also showed that  $^{13}\text{C}_6$ -leucine-labeled SOD1 in the CSF could be measured, that the half-life of CSF SOD1 was on the order of days, and that the kinetics of CSF SOD1 closely paralleled the kinetics of SOD1 in the CNS, specifically the spinal cord. However, the changing plasma-free  $^{13}\text{C}_6$ -leucine enrichment over the time course presented a level of complexity in the system that excluded a simple calculation of SOD1 half-life. Specifically, the linear rise and first-order decay of the curve as well as the persistence of substantial  $^{13}\text{C}_6$ -leucine long after the cessation of labeled diet reflected the slow kinetics of the oral administration method and the contribution of whole-body tracer recycling to long-term kinetic analysis, respectively. As such, we recognized the need to model the system in order to account for the dynamics of this tracer pool and its influence on the tissue-specific SOD1 pools to precisely quantify in vivo SOD1 kinetics.

*Kinetic modeling defined slow SOD1 kinetics.* A compartmental model was developed to account for the shape of the plasma  $^{13}\text{C}_6$ -leucine time course and long-term whole-body tracer recycling (Supplemental Figure 2A). In this model, plasma leucine represents a central compartment in which tracer freely exchanges with all other measured compartments and whole-body protein or is irreversibly lost from the system. From this central compartment, forward arrows indicate the forward exchange of tracer into each tissue compartment (Supplemental Figure 2, A and B). The reverse arrows indicate tracer return and represent the FTR, expressed as pools per day, for each compartment (Supplemental Figure 2, A and B). Best-fit curves for free plasma  $^{13}\text{C}_6$ -leucine and spinal cord, cortex, CSF, liver, and kidney SOD1 are shown overlaid the raw data in Figure 2B. The shape of the plasma  $^{13}\text{C}_6$ -leucine curve during labeling represents the simulated pulsatile nature of oral  $^{13}\text{C}_6$ -leucine tracer administered twice a day for 7 days. The model calculated a half-life of 14.9 days for CSF SOD1, confirming that SOD1 is a relatively long-lived protein in this pool (Table 1). Furthermore, it showed no significant difference between SOD1 turnover rate in the CSF and the spinal cord, suggesting that the CSF pool could serve as a suitable proxy for spinal cord SOD1.

*SOD1 WT and G93A turnover.* Although we were primarily concerned with using SILK to measure the turnover of SOD1 in the CSF and the CNS, our labeling method also allowed us to examine SOD1 turnover in several tissues within the same animal. As expected, the plasma-free  $^{13}\text{C}_6$ -leucine served as the tracer source for all measured SOD1 pools. Interestingly, SOD1 turnover was markedly slower in the CNS (Figure 2B and Table 1). Specifically, the half-life of SOD1

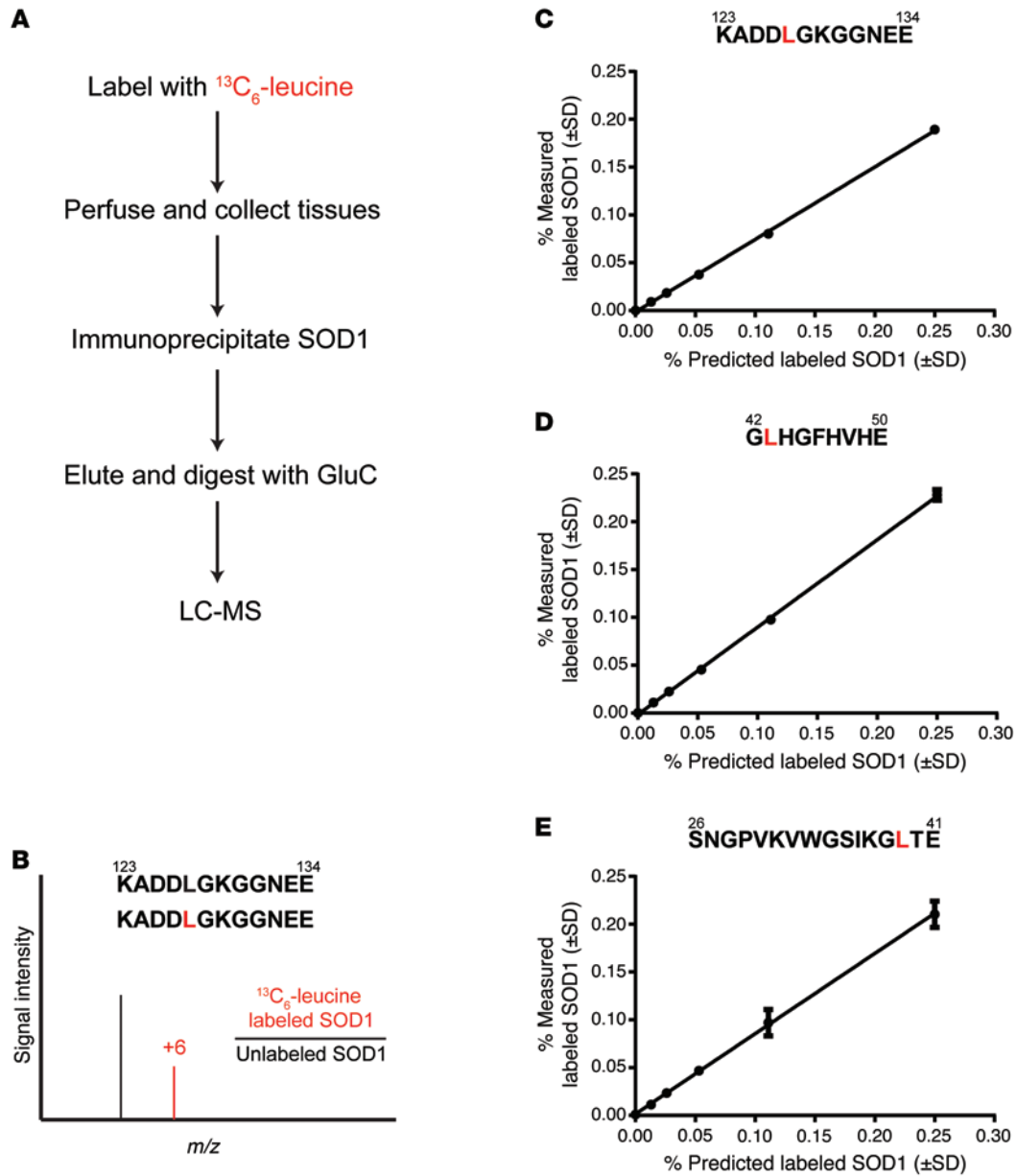


**Figure 1. Schematic of SOD1 isolation and mass spectrometry detection method.** (A) Flow chart detailing the isolation, processing, and detection of leucine-containing SOD1 peptides. GluC, endoproteinase Glu-C; LC-MS, LC/tandem MS. (B) Schematic representing LC/tandem MS detection of <sup>13</sup>C<sub>6</sub>-leucine-containing peptides. The +6-Da shift in the leucine-containing peptide KADDL<sup>13</sup>GKGGNEE reflects the incorporation of <sup>13</sup>C<sub>6</sub>-leucine. (C–E) LC/tandem MS standard curves for the 3 leucine-containing peptides used in quantifying labeled SOD1.

in the spinal cord (15.9 days) and cortex (9.3 days) was 2.8 to 9 times slower than the half-life in the liver (1.8 days) or kidneys (3.4 days).

To better understand disease models, we also applied our SILK method to SOD1 G93A rats (Supplemental Figure 2B and Figure 3A). Similar to SOD1 WT rats, the shape of the plasma-free <sup>13</sup>C<sub>6</sub>-leucine curve confirmed that these animals received sufficient label (Figure 3B). When comparing the SOD1-labeling curves, the same relative differences among tissues with regards to SOD1 turnover rates were evident (Table 1). When comparing between SOD1 WT and G93A in the same tissues, SOD1 G93A had a 1.1- to 1.8-fold faster turnover rate, with the exception of the rate in the kidneys. This accelerated turnover rate for SOD1

G93A agrees with previous cell culture and in vivo studies and may reflect an unstable state (26–30).

In addition to assaying total soluble SOD1 G93A, we were able to immunoprecipitate the pool of misfolded SOD1 G93A from the spinal cord in our labeled animals using the misfolded-specific SOD1 antibody B8H10. Best-fit curves showed that the misfolded G93A pool had much faster turnover rate than total soluble SOD1 G93A in each tissue measured (Figure 3C). Misfolded SOD1 G93A had extremely rapid kinetics in the liver, faster than those of the total soluble SOD1 G93A pool and much faster than those of the misfolded protein pool in the spinal cord. Interestingly, misfolded SOD1 G93A in the liver peaked higher than the peripheral plasma-free <sup>13</sup>C<sub>6</sub>-leucine

**Table 1. Model parameters for SOD1 WT and G93A turnover in ALS rats**

	SOD1 WT			SOD1 G93A		
	FTR (pools/d)	95% CI	Half-life (d)	FTR (pools/d)	95% CI	Half-life (d)
Whole-body protein	0.063	0.057–0.069	11.0	0.089	0.085–0.093	7.8
Liver SOD1	0.397	0.379–0.415	1.7	0.485	0.457–0.514	1.4
Kidney SOD1	0.205	0.197–0.213	3.4	0.188	0.180–0.196	3.7
Cortex SOD1	0.074	0.071–0.078	9.3	0.104	0.098–0.109	6.7
CSF SOD1	0.047	0.044–0.050	14.9	0.074	0.070–0.077	9.4
Spinal cord SOD1	0.044	0.041–0.046	15.9	0.077	0.073–0.081	9.0
Liver misfolded SOD1				0.868	0.795–0.941	0.8
Spinal cord misfolded SOD1				0.325	0.309–0.342	2.1
Liver total protein	1.265	1.121–1.409	0.5	0.711	0.655–0.767	1.0
Cortex total protein	0.177	0.167–0.186	3.9	0.127	0.120–0.135	5.4
Spinal cord total protein	0.087	0.081–0.094	7.9	0.096	0.088–0.104	7.2

The FTR, 95% CI, and half-life were calculated for each compartment in the SOD1 kinetic model. The data confirm the long half-life of SOD1 in CNS tissues, with SOD1 WT approximately 9-fold and 5-fold longer-lived in the spinal cord and cortex than in the liver, respectively. For SOD1 G93A, this relationship persists, with SOD1 approximately 6- and 4.5-fold longer-lived in spinal cord and cortex than in the liver, respectively. Between groups of animals, SOD1 G93A was generally shorter lived in each tissue than SOD1 WT.

enrichment, which likely reflected first-pass absorption of the orally administered tracer coupled with a fast turnover rate. As expected, no misfolded SOD1 could be immunoprecipitated or detected by LC/tandem MS in either spinal cords or livers from SOD1 WT animals (data not shown). These data indicate that misfolded mutant SOD1 is not unique to the spinal cord and that its turnover rate is accelerated relative to total soluble SOD1 and suggest that its low levels in the liver may be a function of its fast turnover rate.

*Determination of SOD1 turnover in human CSF using SILK.* Translating this SILK method to healthy, normal human research participants allowed us to determine CSF SOD1 turnover rates as a proxy for CNS SOD1 turnover rate. In these human studies, we optimized the timing of CSF and blood sampling over a long time period, because our SOD1 WT rodent studies revealed a slow CSF SOD1 turnover rate (approximately 15 days), and the major limitation of the human study was the frequency of CSF collections by lumbar puncture. Human participants consumed a controlled leucine-containing diet supplemented with  $^{13}\text{C}_6$ -leucine powder for 10 days. Plasma and CSF were collected at indicated time points after label administration and processed for plasma-free  $^{13}\text{C}_6$ -leucine, total CSF protein, and labeled SOD1 (Figure 4A). The data were then modeled as previously described, where plasma-free  $^{13}\text{C}_6$ -leucine fit to a central compartment and tracer freely exchanged with all other tissue compartments (Supplemental Figure 2C).

In all subjects, plasma-free  $^{13}\text{C}_6$ -leucine enrichment achieved approximately 3% at the end of label administration. This indicated that our 10-day oral labeling strategy resulted in detectable and sufficient plasma  $^{13}\text{C}_6$ -leucine enrichment for quantifying in vivo CSF SOD1 kinetics in the context of a controlled leucine diet. This was confirmed after quantifying  $^{13}\text{C}_6$ -leucine abundance in CSF total protein (Table 2). For each subject, the CSF SOD1-labeling curve displayed a slow rise and fall relative to total CSF protein labeling, indicating a much slower CSF SOD1 turnover rate of CSF SOD1 compared with that of CSF total protein. The average CSF SOD1 and CSF total protein half-life was  $25.0 \pm 7.4$  days and  $3.6 \pm 1.0$  days, respectively. Thus, the human CSF SOD1 turnover rate agreed with

the slow SOD1 turnover rate observed in our rodent study. Importantly, these 4 human studies validated our  $^{13}\text{C}_6$ -leucine oral administration paradigm for quantifying long-lived protein kinetics.

## Discussion

This approach marks the first time to our knowledge that a stable isotope of an amino acid was administered orally for the purposes of measuring the turnover of a long-lived protein in human CSF and expands the repertoire of oral tracers for studying long-lived proteins in vivo. Similar to oral administration of heavy water, our oral  $^{13}\text{C}_6$ -leucine administration paradigm resulted in detectable amounts of labeled amino acid in the plasma and CSF, suggesting that this approach is reliable and suitable for quantifying protein kinetics in tissues and CSF of animals and humans. The oral SILK approach presents significant advantages. First, oral administration of the tracer amino acid is technically easier than intravenous or intraperitoneal injections in humans or rodents and achieves predictable labeling in plasma and tissue protein pools. Second, it is much safer than using radioactively labeled amino acids. Third, the time scale over which the labeling and tissue collection occurs facilitates the study of other long-lived proteins. Fourth, the LC/tandem MS is highly specific for detecting and quantifying label-incorporated SOD1 peptides after immunoprecipitation and digestion of soluble SOD1. Oral administration of  $^{13}\text{C}_6$ -leucine was well tolerated, with no adverse events reported by the participants (data not shown); achieved detectable levels in both rodents and humans; and displayed predictable kinetics. Isolation and LC/tandem MS detection of tracer-incorporated SOD1 peptides enabled a high degree of specificity as a result of both antibody specificity and predicted  $m/z$  ratios. Overall, this method provides a specific, quantitative, and safe approach for quantifying long-lived protein turnover in vivo, with extensive applications to many areas of biology.

The development of our SILK method allowed us to measure the rate of SOD1 turnover in the CSF of human subjects. After optimization of the method in humans, we found that SOD1 half-life in the CSF was approximately  $25 \pm 7$  days, a number that reflects the long

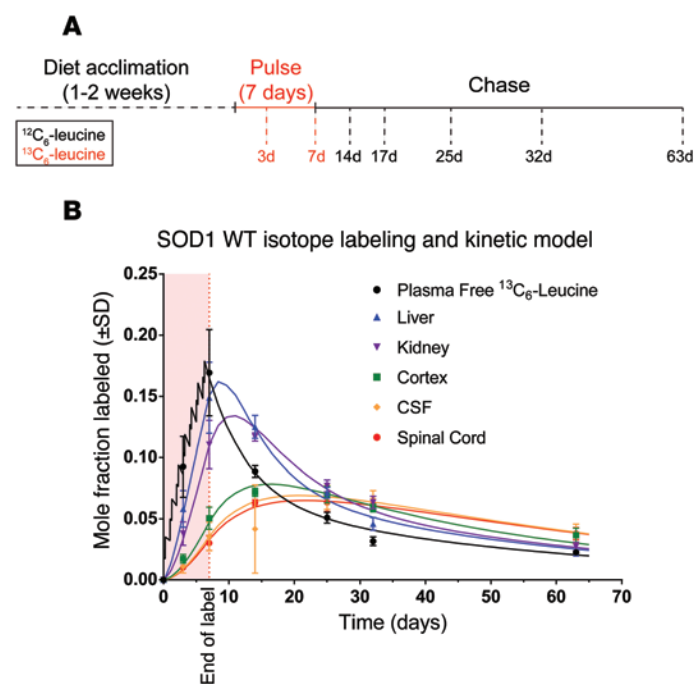


**Figure 2. Kinetic data and model from SOD1 WT rats.** (A) Schematic of the oral labeling paradigm. SOD1 WT rats were fed  $^{13}\text{C}_6$ -leucine for 7 days and then chased with unlabeled leucine for an additional 56 days. Tissues were collected at the indicated time points, and detergent soluble SOD1 was immunoprecipitated, digested, and analyzed by LC/tandem MS. (B) Mole fraction labeled plasma-free  $^{13}\text{C}_6$ -leucine and liver, kidney, cortex, CSF, and spinal cord SOD1 WT were plotted over time (individual points). Solid lines represent best-fit model curves. The shape of the plasma leucine curve during the  $^{13}\text{C}_6$ -leucine-labeling period reflects the pulsatile administration of the tracer twice daily. The slower kinetics of SOD1 WT in spinal cord, cortex, and CSF are reflected in the gradual rise and fall of the curves compared with the steep slopes seen in liver and kidney. Light red shading between 0 and 7 days represents the  $^{13}\text{C}_6$ -leucine-labeling period.  $n = 3$  for all time points with the exception of days 3 and 7 ( $n = 6$ ).

half-life of SOD1 WT in the CSF of transgenic rats. We also found that the half-life of CSF total protein was  $3.6 \pm 1.0$  days. Since the CSF total protein pool is weighted heavily by few abundant proteins, this is not a representative sample of CNS protein pools. However, our rat study did show that CSF and spinal cord SOD1 turnover were not significantly different, suggesting that CSF SOD1 could be used as a proxy for the spinal cord SOD1 pool. Determination of human SOD1 turnover in the CSF has important implications for understanding SOD1 biology in ALS and for biomarker development and monitoring therapy in patients treated with SOD1 ASOs (17, 22, 31). By measuring the half-life of SOD1 in human CSF, one can predict the optimal time to measure SOD1 CSF concentrations in patients treated with SOD1 ASOs. The data also influence the timing and frequency of dosing as well as many other pharmacodynamic aspects of ASO therapy. Indeed, one theoretical application of this technique involves labeling during ASO treatment to monitor therapeutic effects of the drug on SOD1 clearance rates.

Although we have successfully measured SOD1 half-life in healthy subjects, an important future study will need to address mutant SOD1 half-life in patients with ALS. Our rat data and previous cell culture studies confirm that mutant SOD1 half-life is significantly shorter than WT half-life and that the degree of half-life reduction may be mutant dependent (26–29). The autosomal dominant nature of SOD1-ALS means that patients have one copy of both WT and mutant SOD1. A significant advantage in our LC/tandem MS SILK approach is the ability to independently measure both WT and mutant SOD1 species in the same patient, as single amino acid changes result in detectable changes in the  $m/z$  ratios of predicted peptides. Future studies in these patients have the potential to determine SOD1 turnover as a function of age or disease status (e.g., presymptomatic versus symptomatic) and to determine what degree the SOD1 WT half-life is or is not influenced by the presence of mutant SOD1.

In SOD1 WT and G93A rats, the tissues most affected in ALS (i.e., spinal cord and cortex) possessed the slowest rate of turnover. Slow turnover may explain the general susceptibility of the CNS in many neurodegenerative proteinopathies. Indeed, global proteomics approaches using stable isotopes have shown that brain proteins possess a slow turnover rate, even if identical proteins or protein complexes are compared between tissues (4, 32). This relative difference between tissues agrees with our TCA-precipitated total protein data from cortex and liver and suggests, but does not prove, that slower protein turnover in the CNS tissue may result in misfolded SOD1 accumulation and pathology. Consistent with this, in primary culture, slow protein turnover correlates with susceptibility to toxicity (33, 34). As mutant SOD1 selectively kills motor neurons, it will be important to determine the relative rates of SOD1 protein turnover in specific cell types within the CNS.

Our SILK labeling method could be applied to study the kinetics of a wide variety of long-lived proteins in both animal models and human CSF and plasma. We hypothesize that most intracellular proteins in the CNS have a half-life on the order of days to weeks, making them ideal for the long-term labeling method developed here. Our kinetic data from TCA-precipitated total protein from spinal cord and cortex support this claim, with a half-life of 7.9 and 3.9 days for SOD1 WT rats, respectively (Table 1).

It should be noted that  $\text{D}_2\text{O}$  labeling has also been successfully used for understanding kinetics of proteins in the CNS (13). We used oral  $^{13}\text{C}_6$ -leucine in this study because of the known safety of oral leucine and the high enrichment of the label within a single M+6 isotopomer, which facilitates LC/tandem MS analysis.

With this study, we have demonstrated a successful SILK design that uses oral administration of a tracer amino acid for measuring long-lived proteins in rodents and human subjects. This

**Table 2. CSF SOD1 and total protein half-life in human participants**

	Half-life (d)				Average ( $\pm$ SD)
	Subject 1	Subject 2	Subject 3	Subject 4	
CSF total protein	2.4	4.9	3.7	3.45	$3.6 \pm 1.0$
CSF SOD1	19.2	18.3	32.9	29.8	$25.0 \pm 7.4$

Average half-life was calculated for CSF total protein and CSF SOD1.

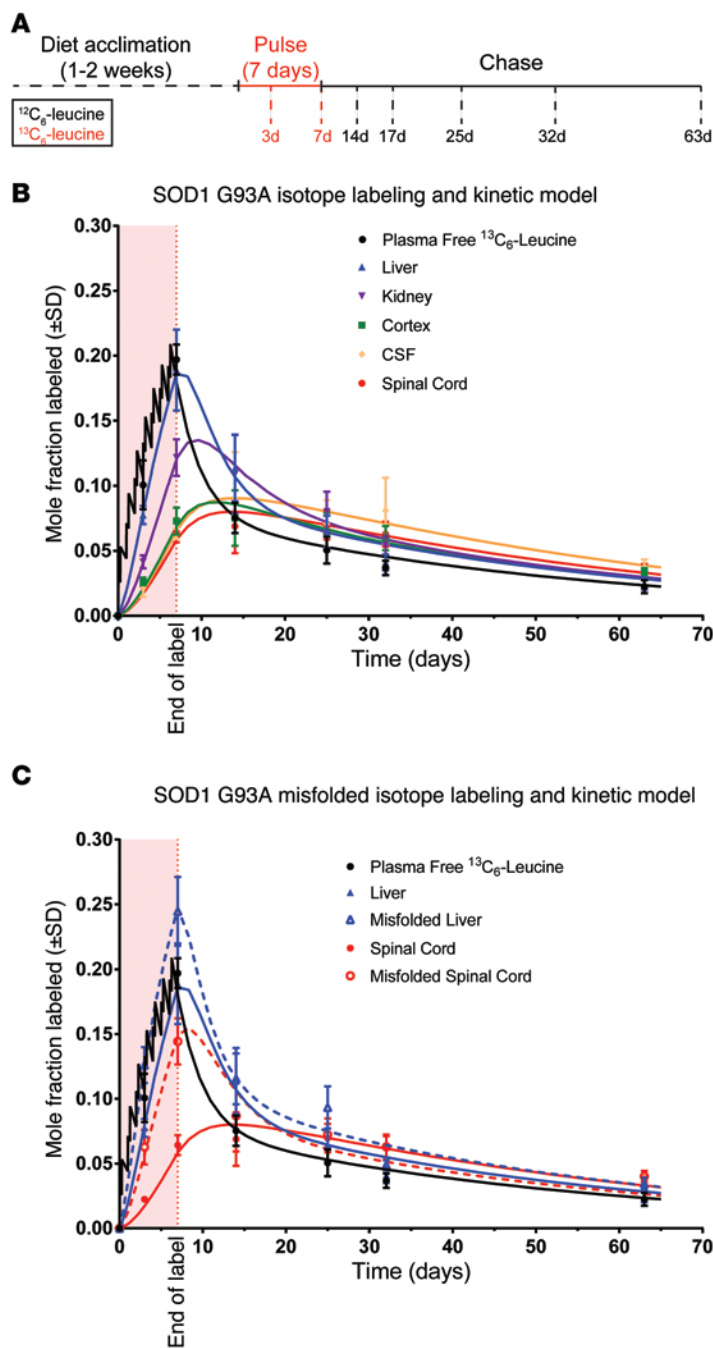


**Figure 3. Kinetic data and model from SOD1 G93A rats. (A)** Schematic of the oral labeling paradigm. SOD1 G93A rats were fed  $^{13}\text{C}_6$ -leucine for 7 days and then chased with unlabeled leucine for an additional 56 days. Tissues were collected at the indicated time points, and detergent soluble SOD1 was immunoprecipitated, digested, and analyzed by LC/tandem MS. **(B)** Mole fraction labeled plasma-free  $^{13}\text{C}_6$ -leucine and liver, kidney, cortex, CSF, and spinal cord SOD1 G93A were plotted over time (individual points) and modeled as previously described (solid lines). The slower kinetics of SOD1 G93A in spinal cord, cortex, and CSF are reflected in the gradual rise and fall of the curves compared with the steep slopes seen in liver and kidney. **(C)** Misfolded SOD1 G93A was immunoprecipitated from previously labeled SOD1 G93A rat tissue with the  $\alpha$ -misfolded SOD1 B8H10 antibody, digested, analyzed by LC/tandem MS, and modeled as previously described (solid lines represent total soluble SOD1; dashed lines represent misfolded SOD1). Labeled misfolded pools in both spinal cord and liver reveal accelerated turnover rates when compared with total soluble SOD1 within each tissue. For both graphs, light red shading between 0 and 7 days represents the  $^{13}\text{C}_6$ -leucine pulse interval.  $n = 3$  for all time points with the exception of day 14 ( $n = 2$ ).

(35, 36). Both labeled L-leucine ( $\text{U-}^{13}\text{C}_6$ , 97%–99%, CLM-2262) and unlabeled L-leucine (ULM-8203) were obtained from Cambridge Isotope Laboratories Inc. and dissolved in water (5 mg/ml). To increase palatability, leucine solutions were sweetened with sucrose (20 mg/ml). During the course of the experiment, rats were fed ad libitum a modified Baker Amino Acid Fiet chow (TestDiet) that contained no leucine. 50 mg leucine (10 ml total volume) was orally administered twice daily (100 mg total daily dose) in accordance with published daily leucine requirements (37). Before administration of the  $^{13}\text{C}_6$ -leucine label, rats were acclimated to the unlabeled leucine diet for 1 to 2 weeks. Rats were then labeled with  $^{13}\text{C}_6$ -leucine for 7 days and chased with unlabeled leucine for an additional 7, 19, 25, or 56 days. At the indicated time points, rats were anesthetized with isoflurane, and approximately 200  $\mu\text{l}$  CSF was extracted from the cisterna magna, flash frozen, and stored at  $-80^\circ\text{C}$ . Rats were then perfused (15 ml/min) with cold PBS containing 0.03% heparin sulfate for 15 minutes. Blood was collected from the mechanically ruptured vena cavae at the start of perfusion and spun at 1,800  $g$  for 10 minutes, and the supernatant was flash frozen and stored at  $-80^\circ\text{C}$ . After perfusion, spinal cords, cortices, livers, and kidneys were harvested, flash frozen in liquid nitrogen, and stored at  $-80^\circ\text{C}$ . Three rats were sacrificed at each collection time point, with the following exceptions: SOD1 WT rats sacrificed at days 3 and 7 ( $n = 6$ ) and SOD1 G93A rats sacrificed at day 14 ( $n = 2$ ).

**Fractionation of tissue lysates.** Tissues were thawed on ice and homogenized in 5 $\times$  v/v of TEN buffer (10 mM Tris, pH 8, 1 mM EDTA, 100 mM NaCl) containing the protease inhibitors AEBSEF, aprotinin, bestatin E-64, leupeptin, and pepstatin A (Sigma-Aldrich P8340). A portion of the tissue lysate was centrifuged at 100,000  $g$  for 10 minutes (Beckman Coulter Optima TLX-120 Ultracentrifuge), and the supernatant was saved for misfolded SOD1 immunoprecipitation. Detergent soluble SOD1 was extracted as described previously (38). Briefly, the homogenate was mixed with an equal volume of 2 $\times$  extraction buffer (10 mM Tris, pH 8, 1 mM EDTA, 100 mM NaCl, 1% NP-40, protease inhibitors), sonicated, and centrifuged at

technique enabled us to show that SOD1 is a long-lived protein in human CSF and that the half-life of SOD1 in the CSF correlates with that in the CNS in rats. The method described here has wide-ranging applications that could be applied to measure protein turnover in a number of neurodegenerative diseases in both animals and human CSF (or plasma) as well as monitor the pharmacodynamics of treatments designed to modulate protein levels, such as ASOs, small molecules, or siRNA.

## Methods

**Stable isotope labeling in rats.**  $^{13}\text{C}_6$ -leucine-labeling experiments were performed in 100-day-old male and female transgenic rats overexpressing human SOD1 WT (provided by Pak Chan, Stanford University, Stanford, California, USA) or SOD1 G93A (Taconic model 2148)

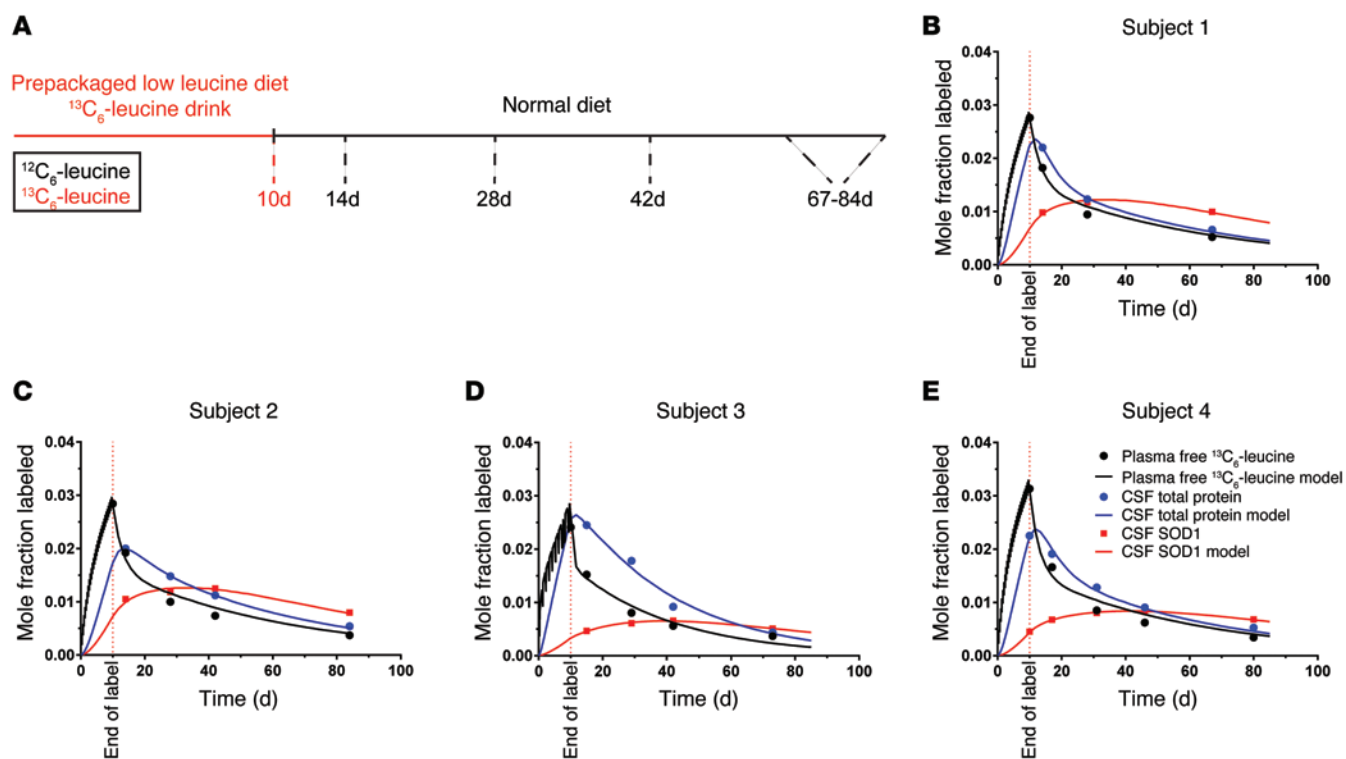


**Figure 4. Modeling SOD1 kinetics in human CSF.** (A) Schematic of the oral labeling paradigm. Participants were placed on a prepackaged low-leucine diet and administered  $^{13}\text{C}_6$ -leucine for 10 days, after which they resumed a normal diet. CSF and plasma were collected at the indicated time points, and total protein and SOD1 were isolated, digested, and analyzed by GC-MS and LC/tandem MS, respectively. (B–E) Data points with overlaid best-fit model curves (solid lines) of plasma-free  $^{13}\text{C}_6$ -leucine, CSF total protein, and CSF SOD1 for human (B) subject 1, (C) subject 2, (D) subject 3, and (E) subject 4.

100,000 *g* for 10 minutes at 4°C. The supernatant, representing the detergent soluble fraction, was transferred to a new tube, and protein concentration was determined by BCA assay (Pierce).

**Preparation of  $^{13}\text{C}_6$ -leucine-labeled SOD1 standard curve.** Labeled (containing  $^{13}\text{C}_6$ -leucine) and unlabeled media were prepared from RPMI-1640 medium without arginine, leucine, lysine, and phenol red (Sigma-Aldrich R-1780) supplemented with 10% dialyzed fetal bovine serum (Sigma-Aldrich F0392), 200 mg/l L-arginine, 40 mg/l lysine, and 50 mg/l of either  $^{13}\text{C}_6$ -leucine (labeled) or unlabeled leucine. HEK293T cells, which constitutively express human SOD1, were used to prepare  $^{13}\text{C}_6$ -leucine-labeled SOD1 standards. Cells were grown to near confluence in complete RPMI-1640 medium supplemented with 10% fetal bovine serum, then split into 10-cm dishes at a low concentration and allowed to settle overnight. Cells were then washed once with PBS and grown to near confluence (approximately 72 hours) in 0%, 0.08%, 0.17%, 0.34%, 0.68%, 1.25%, 2.5%, 5%, 10%, or 20% labeled/unlabeled media. Cells were then washed once with PBS and homogenized in cold lysis buffer (50 mM Tris, pH 8, 150 mM NaCl, 1% NP-40, protease inhibitors) with sonication (20% power for 20 seconds). The lysate was spun at 15,000 *g* for 5 minutes, the supernatant was collected, and protein was quantified using the BCA Protein Assay (Pierce). Aliquots of lysate were frozen at –80°C.

**Isolation and mass spectrometric analysis of  $^{13}\text{C}_6$ -leucine-labeled SOD1, plasma-free  $^{13}\text{C}_6$ -leucine, and  $^{13}\text{C}_6$ -leucine-labeled total protein.** M-270 Epoxy Dynabeads (Invitrogen) were cross-linked to either anti-SOD1 (mouse monoclonal; Sigma-Aldrich S2147) or anti-misfolded SOD1 (B8H10, mouse monoclonal, MédiMabs MM-0070) antibodies using the

Dynabeads Antibody Coupling Kit (Invitrogen) at a concentration of 25  $\mu\text{g}$  antibody per mg of beads. Total soluble SOD1 was immunoprecipitated from the detergent soluble tissue fraction or standard curve HEK293T cell lysate (approximately 100  $\mu\text{g}$  of protein) using 50  $\mu\text{l}$  anti-SOD1 cross-linked Dynabeads overnight in 1X TEN buffer containing 0.1% Tween and protease inhibitors. Misfolded SOD1 was immunoprecipitated from tissue lysates taken prior to detergent fractionation, which had been spun at 100,000 *g*. The beads were washed 3 times in PBS, and SOD1 was eluted from the beads with 50  $\mu\text{l}$  of formic acid. The formic acid eluent was transferred to a new polypropylene tube and lyophilized via speed vacuum (Labconco CentriVap), resuspended with 100% methanol, lyophilized again via speed vacuum, and resuspended in 25  $\mu\text{l}$  of 25 mM  $\text{NaHCO}_3$  buffer (pH 8.8). 600 ng of sequencing-grade endoproteinase Glu-C (Roche) was added to each sample and digestion was allowed to proceed at 25°C for 17 hours. Samples were again lyophilized via vacuum and resuspended in 20  $\mu\text{l}$  5% acetonitrile/0.05% formic acid prior to liquid chromatography–triple quadrupole mass spectrometry (UPLC/tandem MS) analysis (Xevo, Waters). The  $^{13}\text{C}_6$ -leucine/ $^{12}\text{C}_6$ -leucine ratio in SOD1 peptides was quantified by comparing the area under the curve for the SOD1 peptides KADDLKGKGGNEE, GLHGFHVHE, and SNGPVKVVWGSIKGLTE in the presence or absence of  $^{13}\text{C}_6$ -leucine. The full list of transition ions used to acquire the UPLC/tandem MS data is provided in Supplemental Table 1. Excellent correlations among these peptides enabled us to use the peptide with the most robust signal for kinetic analysis (Supplemental Figure 3).

Plasma-free  $^{13}\text{C}_6$ -leucine abundance reflected the precursor pool enrichment for SOD1 protein synthesis. Plasma proteins were

precipitated with 10% trichloroacetic acid overnight at 4°C, the protein pellet was retained for quantification of bound  $^{13}\text{C}_6$ -leucine, and the supernatant was removed after centrifugation at 21,000 *g* for 10 minutes. The supernatant was chemically derivatized to form the *N*-heptafluorobutyl *n*-propyl esters of plasma-free amino acids, and  $^{13}\text{C}_6$ -leucine enrichment was quantified using capillary gas chromatography–negative chemical ionization–quadrupole mass spectrometry (GC-MS; Agilent 6890N Gas Chromatograph and Agilent 5973N Mass Selective Detector) with the *m/z* of 355 as compared with 349 as described previously (11, 39). Protein-bound  $^{13}\text{C}_6$ -leucine abundance was quantified in the TCA-precipitated proteins after sonicating the pellet in a cold 10% TCA solution twice. The pellets were hydrolyzed in 6 N HCl for 24 hours at 110°C. The hydrolysates were subjected to cation-exchange chromatography (50W-X8 resin, Sigma-Aldrich) to trap the protein-bound amino acids that were eluted from the column with 6 N  $\text{NH}_4\text{OH}$ . The samples were then dried under vacuum and processed for GC-MS analysis as described previously (40). Labeled/unlabeled ratios from both the UPLC/tandem MS and GC-MS were obtained as tracer/tracee ratios (TTR) and converted to mole fraction label (MFL) to account for the bias that occurs at high stable tracer enrichments using the following equation:  $MFL = TTR / (1 + TTR)$ .

**Human subjects.** Demographics of the 5 participants are described in Supplemental Table 2. All participants underwent an initial screening visit that consisted of a physical and neurological examination and phlebotomy for a complete blood count, complete metabolic panel, prothrombin time, and partial thromboplastin time. Exclusion criteria included evidence of neurologic disorder by history or examination, inability to safely take food and drink by mouth, lab values greater than 2 times the upper limit of normal, special diets (e.g., gluten free), pregnancy, allergy to lidocaine, history of bleeding disorders, or contraindications for lumbar puncture. Eligible participants consumed a prepackaged reduced leucine diet supplemented with  $^{13}\text{C}_6$ -leucine powder for 10 days. The controlled leucine diet (approximately 2,000 mg leucine per day) was prepared by dietitians in the Washington University Research Kitchen, handed to the subjects, and consumed at home. Food intake was monitored by a self-reported food journal. Participants consumed  $^{13}\text{C}_6$ -leucine (Cambridge Isotope Laboratories CLM-2262) after dissolving 330 mg  $^{13}\text{C}_6$ -leucine and Kool-Aid–flavored powder in 120 ml tap water 3 times per day (total daily dose = 990 mg). During the  $^{13}\text{C}_6$ -leucine-labeling period, overnight fasting blood was collected on days 1 and 10 of the research meal plan. On day 11, participants resumed consumption of their habitual diets. CSF (via lumbar puncture) and venous blood samples were collected approximately 14, 28, 42, and 67–84 days after  $^{13}\text{C}_6$ -leucine-labeling was initiated (actual time points differed slightly among subjects). Approximately 20 to 25 ml of CSF was drawn with each lumbar puncture.

Blood was centrifuged at 1,800 *g* for 10 minutes, and the serum was aliquoted into low-binding 1.5-ml tubes (Ambion AM12450), frozen on dry ice, and stored at –80°C. CSF (20–25 ml) was centrifuged at 1,000 *g* for 10 minutes at 4°C, and 1 ml was aliquoted into several low-binding 1.5-ml tubes, frozen on dry ice, and stored at –80°C. Immunoprecipitation of SOD1 from 1 ml CSF was carried out by adding 50  $\mu\text{l}$  anti-SOD1 cross-linked M-270 Dynabeads, protease inhibitors, and Tween (final concentration 0.1%) and rotating the tubes overnight at 4°C. SOD1 was eluted from the beads (99% 50  $\mu\text{l}$  formic acid), digested (endoproteinase Glu-C), and prepared for LC/tandem MS analysis as described above for rodent CSF. Plasma-free  $^{13}\text{C}_6$ -leucine enrichment was quantified as described

above and used to reflect the precursor pool enrichment for SOD1 protein synthesis.  $^{13}\text{C}_6$ -leucine abundance in human plasma (50  $\mu\text{l}$ ) and CSF (1 ml) protein precipitates (10% TCA) was quantified as described above.

**Compartmental modeling of rodent and human kinetic data.** Modeling was conducted using SAAM II (Resource for Kinetic Analysis, University of Washington, Seattle, Washington, USA). For the animal studies, the kinetic data for plasma-free  $^{13}\text{C}_6$ -leucine, tissue-specific SOD1 species, and total protein from liver, cortex, and spinal cord were incorporated into a compartmental model. The KADDLGKGGNEE peptide was used for modeling, as it had the most robust LC/tandem MS signal. The model consisted of a central plasma leucine compartment that initially received the orally administered tracer and which exchanged tracer-labeled leucine with all proteins throughout the body (Supplemental Figure 2, A and B). Arrows connecting the compartments of the model represent first-order rate constants (units: pools per day) that describe the flux of leucine between compartments (Supplemental Figure 2, A and B). The model describes the complete time course of tracer incorporation and clearance into each measured compartment; the FTR (pools per day) for each compartment is the rate constant for the return of leucine from each compartment back to plasma. Note that isotopic enrichment time course data were available for plasma leucine and for all protein/tissue compartments highlighted in Supplemental Figure 2, A and B. A “whole-body protein” compartment was used to account for most of the shape information of plasma leucine, as label exchanged with all other unsampled proteins. The SAAM program devised first-order linear differential equations, as dictated by the structure of the model, and optimized the fit of the model-projected solution to the data for all sampled protein/tissue compartments simultaneously by adjusting the model rate constants through an iterative process. The model was set up in SAAM in a manner to simulate the appearance of label into plasma as a result of the twice-daily tracer-dosing scheme for the 7 days of oral tracer labeling. A similar model was used for the human studies to account for plasma-free  $^{13}\text{C}_6$ -leucine, CSF total protein, and CSF SOD1 species for each subject following 10 days of thrice-daily oral tracer administration (Supplemental Figure 2C). The GLHGFHVHE peptide gave the most robust LC/tandem MS signal for the human *in vivo* tracer kinetics and was therefore used for modeling. Like the animal model, the central compartment consisted of plasma leucine from which tracer was exchanged with all other compartments. Half-life was calculated as  $\ln 2 / \text{FTR}$ .

**Statistics.** Descriptive statistics for variables in each kinetic model described in this manuscript (FTR, 95% CIs) were calculated using the SAAM II modeling software.

**Study approval.** Animal protocols were approved by the Institutional Animal Care and Use Committee at Washington University and conducted according to the NIH *Guide for the Care and Use of Laboratory Animals* (8th ed. The National Academies Press, 2011.). Studies involving human subjects were approved by the Washington University Human Studies Committee and the Clinical Research Unit Advisory Committee (an Institute of Clinical and Translational Sciences resource unit). Written informed consent was received from all participants prior to inclusion in the study.

## Acknowledgments

We thank Carey Shaner, Amy Wegener, and Tao Shen for expert technical assistance. SOD1 WT rats were provided by Pak Chan, Stanford University. We also thank Lucy Liu and Ling Munsell for their preliminary work on this project and Rebecca Blair for design-

ing and implementing the controlled leucine diet for the human study. Funding was provided by the ALS Association (2427), the NIH (R01NS078398, U01NS084970, and R21NS072584), Washington University Hope Center for Neurologic Disorders Pilot Project (to Timothy M. Miller), and NIH grant 5F31NS078818-02 (to Matthew J. Crisp). Support for clinical subjects was provided by US Public Health Service grant 5UL1 RRO24992-02 to the Center for Applied Research Sciences at Washington University. This study was funded by grants from the NIH (R01NS065667 to Randall J. Bateman) and the Adler Foundation (to Randall J. Bateman) and also supported by the Glenn Foundation (to Randall J. Bateman) and Ruth K. Broadman Biomedical Research Foundation (to Randall J. Bateman). The

Washington University Biomedical Mass Spectrometry Research Facility was funded by NIH grants P41 GM103422, P30 DK056341, and P30 DK020579 to Kevin E. Yarasheski. Bruce W. Patterson gets salary support from the National Institute of Diabetes and Digestive and Kidney Diseases–supported Nutrition Obesity Research Centers (grant P30 DK056341).

Address correspondence to: Timothy M. Miller or Randall J. Bateman, Washington University School of Medicine, Box 8111, 660 South Euclid Avenue, St. Louis, Missouri 63110, USA. Phone: 314.362.8169; E-mail: millert@neuro.wustl.edu (T.M. Miller). Phone: 314.747.7066; E-mail: batemanr@wustl.edu (R.J. Bateman).

- Kiernan MC, et al. Amyotrophic lateral sclerosis. *Lancet*. 2011;377(9769):942–955.
- Worms PM. The epidemiology of motor neuron diseases: a review of recent studies. *J Neurol Sci*. 2001;191(1):3–9.
- Cheah BC, Vucic S, Krishnan AV, Kiernan MC. Riluzole, neuroprotection and amyotrophic lateral sclerosis. *Curr Med Chem*. 2010;17(18):1942–119.
- Price JC, Guan S, Burlingame A, Prusiner SB, Ghaemmaghami S. Analysis of proteome dynamics in the mouse brain. *Proc Natl Acad Sci U S A*. 2010;107(32):14508–14513.
- Bateman RJ, Munsell LY, Morris JC, Swarm R, Yarasheski KE, Holtzman DM. Human amyloid- $\beta$  synthesis and clearance rates as measured in cerebrospinal fluid in vivo. *Nat Med*. 2006;12(7):856–861.
- Bateman RJ, Munsell LY, Chen X, Holtzman DM, Yarasheski KE. Stable isotope labeling tandem mass spectrometry (SILT) to quantify protein production and clearance rates. *J Am Soc Mass Spectrom*. 2007;18(6):997–1006.
- Elbert DL, Mawuenyega KG, Scott EA, Wildsmith KR, Bateman RJ. Stable isotope labeling tandem mass spectrometry (SILT): integration with peptide identification and extension to data-dependent scans. *J Proteome Res*. 2008;7(10):4546–4556.
- Bateman RJ, et al. A  $\gamma$ -secretase inhibitor decreases amyloid-beta production in the central nervous system. *Ann Neurol*. 2009;66(1):48–54.
- Mawuenyega KG, et al. Decreased clearance of CNS  $\beta$ -amyloid in Alzheimer's disease. *Science*. 2010;330(6012):1774.
- Castellano JM, et al. Human apoE isoforms differentially regulate brain amyloid- $\beta$  peptide clearance. *Sci Transl Med*. 2011;3(89):89ra57.
- Potter R, et al. Increased in vivo amyloid- $\beta$ 42 production, exchange, and loss in presenilin mutation carriers. *Sci Transl Med*. 2013;5(189):189ra177.
- Mawuenyega KG, Kastan T, Sigurdson W, Bateman RJ. Amyloid- $\beta$  isoform metabolism quantitation by stable isotope-labeled kinetics. *Anal Biochem*. 2013;440(1):56–62.
- Fanara P, et al. Cerebrospinal fluid-based kinetic biomarkers of axonal transport in monitoring neurodegeneration. *J Clin Invest*. 2012;122(9):3159–3169.
- Price JC, et al. Measurement of human plasma proteome dynamics with (2)H(2)O and liquid chromatography tandem mass spectrometry. *Anal Biochem*. 2012;420(1):73–83.
- Rosen DR, et al. Mutations in Cu/Zn superoxide dismutase gene are associated with familial amyotrophic lateral sclerosis. *Nature*. 1993;362(6415):59–62.
- McCord JM, Fridovich I. Superoxide dismutase. An enzymic function for erythrocyte (hemocuprein). *J Biol Chem*. 1969;244(22):6049–6055.
- Miller TM, et al. An antisense oligonucleotide against SOD1 delivered intrathecally for patients with SOD1 familial amyotrophic lateral sclerosis: a phase 1, randomised, first-in-man study. *Lancet Neurol*. 2013;12(5):435–442.
- Foust KD, et al. Therapeutic AAV9-mediated suppression of mutant SOD1 slows disease progression and extends survival in models of inherited ALS. *Mol Ther*. 2013;21(12):2148–2159.
- Wang H, et al. Widespread spinal cord transduction by intrathecal injection of rAAV delivers efficacious RNAi therapy for amyotrophic lateral sclerosis. *Hum Mol Genet*. 2014;23(3):668–681.
- Liu HN, et al. Targeting of monomer/misfolded SOD1 as a therapeutic strategy for amyotrophic lateral sclerosis. *J Neurosci*. 2012;32(26):8791–8799.
- Gros-Louis F, Soucy G, Lariviere R, Julien JP. Intracerebroventricular infusion of monoclonal antibody or its derived Fab fragment against misfolded forms of SOD1 mutant delays mortality in a mouse model of ALS. *J Neurochem*. 2010;113(5):1188–1199.
- Winer L, et al. SOD1 in cerebral spinal fluid as a pharmacodynamic marker for antisense oligonucleotide therapy. *JAMA Neurol*. 2013;70(2):201–207.
- Ong SE. The expanding field of SILAC. *Anal Bioanal Chem*. 2012;404(4):967–976.
- Gurney ME, et al. Motor neuron degeneration in mice that express a human Cu,Zn superoxide dismutase mutation. *Science*. 1994;264(5166):1772–1775.
- Aoki M, Kato S, Nagai M, Itoyama Y. Development of a rat model of amyotrophic lateral sclerosis expressing a human SOD1 transgene. *Neuropathology*. 2005;25(4):365–370.
- Borchelt DR, et al. Superoxide dismutase 1 with mutations linked to familial amyotrophic lateral sclerosis possesses significant activity. *Proc Natl Acad Sci U S A*. 1994;91(17):8292–8296.
- Hoffman EK, Wilcox HM, Scott RW, Siman R. Proteasome inhibition enhances the stability of mouse Cu/Zn superoxide dismutase with mutations linked to familial amyotrophic lateral sclerosis. *J Neurol Sci*. 1996;139(1):15–20.
- Ratovitski T, et al. Variation in the biochemical/biophysical properties of mutant superoxide dismutase 1 enzymes and the rate of disease progression in familial amyotrophic lateral sclerosis kindreds. *Hum Mol Genet*. 1999;8(8):1451–1460.
- Johnston JA. Formation of high molecular weight complexes of mutant Cu,Zn-superoxide dismutase in a mouse model for familial amyotrophic lateral sclerosis. *Proc Natl Acad Sci U S A*. 2000;97(23):12571–12576.
- Oeda T, et al. Oxidative stress causes abnormal accumulation of familial amyotrophic lateral sclerosis-related mutant SOD1 in transgenic *Caenorhabditis elegans*. *Hum Mol Genet*. 2001;10(19):2013–2023.
- DeVos SL, Miller TM. Antisense oligonucleotides: treating neurodegeneration at the level of RNA. *Neurotherapeutics*. 2013;10(3):486–497.
- Savas JN, Toyama BH, Xu T, Yates JR, Yates JR 3rd, Hetzer MW. Extremely long-lived nuclear pore proteins in the rat brain. *Science*. 2012;335(6071):942.
- Tsvetkov AS, et al. Proteostasis of polyglutamine varies among neurons and predicts neurodegeneration. *Nat Chem Biol*. 2013;9(9):586–592.
- Barmada SJ, et al. Autophagy induction enhances TDP43 turnover and survival in neuronal ALS models. *Nat Chem Biol*. 2014;10(8):677–685.
- Nagai M, et al. Rats expressing human cytosolic copper-zinc superoxide dismutase transgenes with amyotrophic lateral sclerosis: associated mutations develop motor neuron disease. *J Neurosci*. 2001;21(23):9246–9254.
- Chan PH, et al. Overexpression of SOD1 in transgenic rats protects vulnerable neurons against ischemic damage after global cerebral ischemia and reperfusion. *J Neurosci*. 1998;18(20):8292–8299.
- Owens FN, Shin IS, Pettigrew JE, Oltjen JW. Apportioning leucine requirements for maintenance versus growth for rats. *Nutr Res*. 1994;14(1):73–82.
- Prudencio M, Durazo A, Whitelegge JP, Borchelt DR. An examination of wild-type SOD1 in modulating the toxicity and aggregation of ALS-associated mutant SOD1. *Hum Mol Genet*. 2010;19(24):4774–4789.
- Reeds DN, Cade WT, Patterson BW, Powderly WG, Klein S, Yarasheski KE. Whole-body proteolysis rate is elevated in HIV-associated insulin resistance. *Diabetes*. 2006;55(10):2849–2855.
- Parise G, Mihic S, MacLennan D, Yarasheski KE, Tarnopolsky MA. Effects of acute creatine monohydrate supplementation on leucine kinetics and mixed-muscle protein synthesis. *J Appl Physiol*. 2001;91(3):1041–1047.